

Winding Topology of Multifold Exceptional Points

Tsuneaya Yoshida,^{1,2,*} J. Lukas K. König,^{3,†} Lukas Rødland,^{3,‡} Emil J. Bergholtz,^{3,§} and Marcus Stålhammar^{4,5,6,¶}

¹*Department of Physics, Kyoto University, Kyoto 606-8502, Japan*

²*Institute for Theoretical Physics, ETH Zurich, 8093 Zurich, Switzerland*

³*Department of Physics, Stockholm University, AlbaNova University Center, 10691 Stockholm, Sweden*

⁴*Nordita, KTH Royal Institute of Technology and Stockholm University,
Hannes Alfvéns väg 12, SE-106 91 Stockholm, Sweden*

⁵*Institute for Theoretical Physics, Utrecht University,
Princetonplein 5, 3584CC Utrecht, The Netherlands*

⁶*Department of Physics and Astronomy, Uppsala University, Uppsala, Sweden*

(Dated: January 30, 2025)

Despite their ubiquity, a systematic classification of multifold exceptional points, n -fold spectral degeneracies (EPns), remains a significant unsolved problem. In this article, we characterize the Abelian eigenvalue topology of generic EPns and symmetry-protected EPns for arbitrary n . The former and the latter emerge in a $(2n - 2)$ - and $(n - 1)$ -dimensional parameter space, respectively. By introducing topological invariants called resultant winding numbers, we elucidate that these EPns are stable due to topology of a map from a base space (momentum or parameter space) to a sphere defined by resultants. In a D -dimensional parameter space ($D \geq c$), the resultant winding number topologically characterize a $(D - c)$ -dimensional manifold of generic [symmetry-protected] EPns whose codimension is $c = 2n - 2$ [$c = n - 1$]. Our framework implies fundamental doubling theorems for both generic EPns and symmetry-protected EPns in n -band models.

I. INTRODUCTION

The discovery of topological semimetals is one of the significant successes in modern condensed matter physics. A prime example is a Weyl semimetal [1–5] realized in TaAs [6–8] which hosts elementary excitations with linear dispersion analogous to Weyl fermions [9]. For the emergence of Weyl fermions in solids [6–8, 10–12], topologically protected two-band touching in three dimensions plays an essential role which induces negative magnetoresistance. Remarkably, considering more than two bands further enriches the topological semimetals and allows for exotic particles that have no high-energy analogue [13–17]. Specifically, multifold fermions emerge which are described by topologically protected multiband touching points. These particles are extensively studied [18–23] and three-, four-, and six-fold fermions are realized in materials so far [24–27].

Recently, studies on non-Hermitian systems have opened up a new research direction of topological physics [28–53]. One of the unique phenomena is the emergence of exceptional points (EPs) which are band-touching points of both real and imaginary parts accompanied by the coalescence of eigenvectors [54]. Such non-Hermitian band touching is stable in two dimensions and is protected by non-Hermitian topology which is characterized by winding of complex energy eigenvalues [55–57], i.e., Abelian topology. Considering multiband also

enriches EPs [58–65]. Generic n -fold EPs (EPns) in the absence of symmetry emerge in $2n - 2$ dimensions; they require tuning $2n - 2$ parameters [55, 57, 66–74], which is a strikingly small number given that generic n -fold Hermitian band touching requires $n^2 - 1$ tuning parameters [75]. In the presence of parity-time (PT) symmetry, this number is further reduced to $n - 1$ [56, 76–84]. In addition, EPns in multiband systems may exhibit non-Abelian topology [62, 63] [e.g., non-Abelian charge (braiding) of EP2s in systems with three or more bands]. The emergence of EPns is ubiquitous and has been reported for a variety of systems [59, 85–97], such as photonic systems [85–88, 98, 99] and open quantum systems [89, 90] and so on.

Despite their ubiquity, systematic topological characterization of EPns remains a crucial unsolved issue; only symmetry-protected EP3s are characterized so far [59, 97]. One theoretical challenge lies in missing topological invariants characterizing EPns for arbitrary n which quantify their robustness.

In this paper, we systematically characterize the Abelian topology of both generic and symmetry-protected EPns [see Table I]. Through a proper choice of resultants, we generalize resultant winding numbers [59]. In a D -dimensional parameter space with $D \geq c$, our resultant winding number characterize a $(D - c)$ -dimensional manifold of generic [symmetry-protected] EPns, whose codimension is $c = 2n - 2$ [$c = n - 1$]. The characterization of the symmetry-protected EPn is straightforwardly extended to systems with pseudo-Hermiticity, charge-conjugation-parity (CP), or chiral symmetry. Furthermore, the introduced resultant winding numbers lead to doubling theorems of EPns in n -band systems.

The rest of this paper is organized as follows. In Sec. II,

* yoshida.tsuneaya.2z@kyoto-u.ac.jp

† lukas.konig@fysik.su.se

‡ lukas.rodland@fysik.su.se

§ emil.bergholtz@fysik.su.se

¶ marcus.backlund@physics.uu.se

we illustrate our argument of the topological characterization and the doubling theorem for generic EP3s in four dimensions. Generalizing this argument, we address the topological characterization of EP n for arbitrary n ; Secs. III and IV address the case of generic EP n and symmetry-protected EP n , respectively. Sec. V provides a short summary and outlook. The Supplemental Material (SM) is devoted to technical details of resultants; we show equivalence between zero resultant vectors and EP n s in SM Sec. S1, compute the resultant winding number for an acoustic system in SM Sec. S2, provide a generic toy model for EP n s in SM Sec. S3, and explicitly calculate the resultant winding of models with an arbitrary winding number in SM Sec. S4.

II. EP3S IN FOUR DIMENSIONS

We illustrate our arguments for generic EP3s which are robust against perturbations in four dimensions. First, we introduce the resultant vector and the associated topological invariant, the resultant winding number. Then, we provide toy models for EP3s with arbitrary winding numbers. Finally, we provide a fermion doubling theorem for EP3s in a four-dimensional BZ.

A. Resultants and their winding

Since the essential features of an EP3 are captured by a 3×3 -Jordan block [100], we consider a generic non-Hermitian Hamiltonian of a 3×3 -matrix $H(\mathbf{k})$ in the four-dimensional space parameterized by $\mathbf{k} = (k_1, \dots, k_4)^T$. The corresponding eigenvalues are obtained as roots of the characteristic polynomial $P(\lambda, \mathbf{k}) = \det[H(\mathbf{k}) - \lambda \mathbb{1}]$ ($\lambda \in \mathbb{C}$) with $\mathbb{1}$ being the 3×3 identity matrix. Here,

Symmetry	c	Winding Number	Resultants \mathbf{R}
none	$2n - 2$	Eq. (11)	Eq. (8)
PT psH	$n - 1$	Eq. (20)	Eq. (17) with H'
CP CS			

TABLE I. EP n s in c dimensions and the winding numbers characterizing their Abelian topology. “ PT ” and “ CP ” denote parity-time symmetry and charge-conjugation-parity symmetry, respectively. “psH” and “CS” denote pseudo-Hermiticity and chiral symmetry, respectively. A generic (symmetry-protected) EP n emerges in $c = 2n - 2$ ($c = n - 1$) dimensions. These EP n s are characterized by winding numbers of resultants which are specified by the third and fourth columns. In the presence of symmetry, resultants are computed from the characteristic polynomial $P(\lambda) = \det[H' - \lambda \mathbb{1}]$ with $H' = H$ ($H' = iH$) for cases with “ PT ” or “psH” (“ CP ” or “CS”). In this table, c denotes the codimension of EP n s. Namely, in D dimensions ($D \geq c$), EP n s form a $(D - c)$ -dimensional manifold. For systems of m bands ($m > n$), the characterization is done by analyzing the effective $n \times n$ -Hamiltonian which describes n -band touching.

$P(\lambda)$ is a polynomial of degree three. We suppose that three bands touch at \mathbf{k}_0 in four dimensions with energy $\epsilon_0 \in \mathbb{C}$. In this case, the characteristic polynomial has a triple root $P(\lambda, \mathbf{k}_0) = (\lambda - \epsilon_0)^3$. The triple root is captured by vanishing resultants $r_j = 0$ ($j = 1, 2$), where r_j is defined as [101]

$$r_j(\mathbf{k}) = \text{Res} \left[\partial_\lambda^{2-j} P(\lambda, \mathbf{k}), \partial_\lambda^2 P(\lambda, \mathbf{k}) \right] \quad (1)$$

(for more details, see Sec. S1 of SM [102]). In other words, a generic EP3 is captured by the resultant vector

$$\mathbf{R}(\mathbf{k}) = \left(\text{Re}[r_1], \text{Im}[r_1], \text{Re}[r_2], \text{Im}[r_2] \right)^T, \quad (2)$$

which vanishes at EP3s in four dimensions. This argument indicates that the codimension of generic EP3s is $c = 4$, meaning that generic EP3s forms a $D - 4$ manifold in a D -dimensional parameter space ($D \geq 4$).

To quantify the stability of generic EP3s, we introduce the resultant winding number. We consider a three-dimensional sphere surrounding an EP3 in the momentum space and specify a point on the sphere by $\mathbf{p} = (p_1, p_2, p_3)^T$. On this sphere, the resultant vector remains finite and can thus be normalized to $\mathbf{n} = \mathbf{R}/\sqrt{\mathbf{R} \cdot \mathbf{R}}$. This normalized vector induces a map $\mathbf{n}: S^3 \rightarrow S^3$ with $\mathbf{p} \mapsto \mathbf{n}(\mathbf{p})$, which may possess nontrivial topology classified as

$$\pi_3(S^3) = \mathbb{Z} \quad (3)$$

(see Sec. 4.1 of Ref. [103]). The topology is characterized by winding number W_3 [104] [105]

$$W_3 = \frac{\epsilon^{ijkl}}{2\pi^2} \int d^3\mathbf{p} f_{ijkl}, \quad (4)$$

$$f_{ijkl} = n_i \partial_1 n_j \partial_2 n_k \partial_3 n_l,$$

with the anti-symmetric tensor ϵ^{ijkl} satisfying $\epsilon^{1234} = 1$. Here, ∂_μ ($\mu = 1, 2, 3$) denotes the derivative with respect to p_μ .

Reference [96] reports that a coupled acoustic cavity system hosts an EP3 in four dimensions whose topological characterization remains unclear. Computing the resultant winding number elucidates that this EP3 is characterized by $W_3 = 1$ which explicitly clarifies its stability. The details of the system are provided in Sec. S2 of SM [102].

B. Toy models of generic EP3

To explicitly demonstrate the emergence of a topologically protected EP3 in four dimensions, we consider the non-Hermitian Hamiltonian

$$H(\mathbf{k}) = \begin{pmatrix} 0 & 1 & 0 \\ 0 & 0 & 1 \\ z_2 & z_1 & 0 \end{pmatrix}, \quad (5)$$

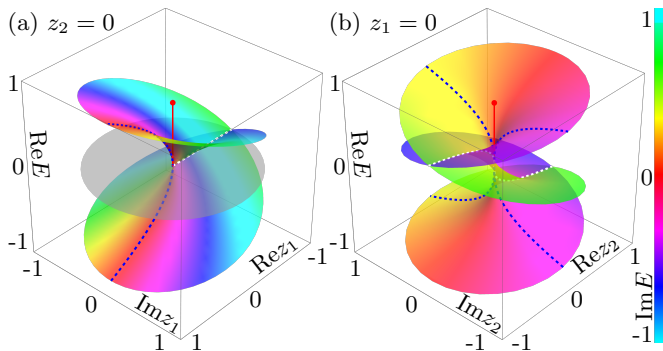


FIG. 1. Cuts of the spectrum of the Hamiltonian (5) showcasing the EP3 at the origin. The real (imaginary) part of the eigenvalues is represented as height (color). Fermi arcs, i.e., coincidences of two eigenvalues’ real (imaginary) parts are shown as white (blue) dashed lines. The panels (a) and (b) show the parameter subspace of $z_2 = 0$ and $z_1 = 0$, respectively.

with $z_1 = k_1 + ik_2$ and $z_2 = k_3 + ik_4$. As shown in Fig. 1, this model hosts an EP3 at $\mathbf{k}_0 = 0$ in four dimensions. The resultant vector of this model is computed as

$$\mathbf{R}(\mathbf{k}) = 36(k_1, k_2, 6k_3, 6k_4), \quad (6)$$

for computation of a general case, see Sec. S3 of SM [102]. Evaluating the integral of Eq. (4), we obtain the winding number $W_3 = 1$. This result is to be expected since the map defined in Eq. (6) is obtained from the identity map via rescaling and the restriction to the sphere.

Models with a higher value of W_3 are obtained by taking powers of z ’s. For instance, the replacement $z_1 \rightarrow z_1^2 = k_1^2 - k_2^2 + 2ik_1k_2$ yields a toy model with $W_3 = 2$. Similarly, complex conjugation $z_1 = k_1 + ik_2 \rightarrow z_1^* = k_1 - ik_2$ in Eq. (5) yields a toy model with $W_3 = -1$.

Finally, we give a prescription for locating EP3s in a three-dimensional context because an EP3 does not necessarily emerge at the specific point $\mathbf{k} = 0$. EP3s are generally surrounded by more abundant EP2s. Fixing one parameter, e.g., k_4 , one is left with a three-dimensional model $H(\mathbf{k})$ that generally contains lines of EP2s. The EP3 can then be regarded as a crossing point of two such lines, on each of which different pairs of bands touch [see Fig. 2]. Such a crossing point can be clearly identified in a parametric sweep of k_4 .

C. Doubling theorem

Having introduced the three-dimensional resultant winding number, we derive a concomitant doubling theorem for EP3s in three-band models, which is a direct consequence of the Poincaré-Hopf theorem [106, 107]. We suppose that there exists an arbitrary number of discrete EP3s labeled by $I = 1, 2, \dots$ in a four-dimensional Brillouin zone (BZ). Then, the summation of all their corresponding winding numbers vanishes $\sum_I W_{3I} = 0$, since

this sum is computed as

$$\sum_I \epsilon^{ijkl} \int_{S_I^3} d^3\mathbf{p} f_{ijkl} = \epsilon^{ijkl} \int_{\partial\text{BZ}} d^3\mathbf{p} f_{ijkl} = 0, \quad (7)$$

up to a common prefactor. Here, S_I^3 denotes a three-dimensional sphere surrounding I -th EP3, and the “boundary” [108] of the four-dimensional BZ is denoted by ∂BZ . The second equal sign is obtained from the periodicity and the orientability of the BZ. This constitutes the doubling theorem: an EP3 with $W_3 = 1$ must be accompanied by an EP3 with $W_3 = -1$ in the BZ.

III. GENERIC EP n IN $2n - 2$ DIMENSIONS

The above argument is straightforwardly generalized to EP n s in $2n - 2$ dimensions. We describe general n -fold band touching by an $n \times n$ non-Hermitian Hamiltonian $H(\mathbf{k})$. From the characteristic polynomial $P(\lambda, \mathbf{k}) = \det[H(\mathbf{k}) - \lambda\mathbb{1}]$ of degree n , we obtain the resultant vector of $2n - 2$ components as

$$\mathbf{R}(\mathbf{k}) = \left(\text{Re}[r_1], \text{Im}[r_1], \dots, \text{Re}[r_{n-1}], \text{Im}[r_{n-1}] \right)^T, \quad (8)$$

$$r_j(\mathbf{k}) = \text{Res}[\partial_\lambda^{(n-1-j)} P(\lambda, \mathbf{k}), \partial_\lambda^{(n-1)} P(\lambda, \mathbf{k})]. \quad (9)$$

An n -tuple root of $P(\lambda)$ corresponds to the vanishing resultant vector, $\mathbf{R}(\mathbf{k}_0) = 0$, which amounts to $2n - 2$ constraints. Thus, the codimension of generic EP n s is $c = 2n - 2$. Namely, a generic EP n in $2n - 2$ dimensions is a point stable against perturbations. In D dimensions ($D > 2n - 2$), EP n s form a $(D - 2n + 2)$ -dimensional manifold [59, 60].

As is the case of EP3s in four dimensions, EP n s in $2n - 2$ dimensions ($n = 2, 3, 4, \dots$) may possess nontrivial topology of the map from the $(2n - 3)$ -dimensional sphere around the EP n in the parameter space to the $(2n - 2)$ -dimensional normalized resultant vector $\mathbf{n} = \mathbf{R}/\sqrt{\mathbf{R} \cdot \mathbf{R}}$. Such maps are topologically classified as (see Sec. 4.1 of

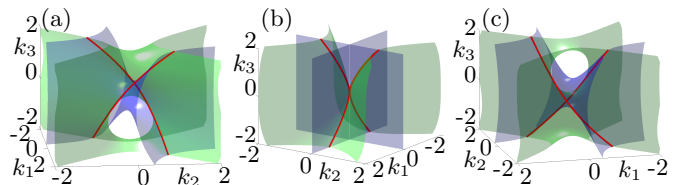


FIG. 2. A generic EP3 visualized as a crossing point of the concomitant lines of EP2s in three dimensions. The green (blue) surfaces denote the real (imaginary) part of the discriminant of the characteristic polynomial of the model in Eq. (5). The data for $k_4 = -1, 0, 1$ are displayed in panels (a), (b), and (c), respectively. The lines of EP2s appear as band touching between different pairs of bands. In panel (b), the two lines of EP2s intersect with each other at an EP3, making a transition from over-crossing to under-crossing or vice versa.

Ref. [103])

$$\pi_{2n-3}(S^{2n-3}) = \mathbb{Z} \quad (10)$$

where the invariant is characterized by winding number W_{2n-3}

$$\begin{aligned} W_{2n-3} &= \frac{\epsilon^{i_1 \dots i_{2n-2}}}{A_{2n-3}} \int d^{2n-3} \mathbf{p} f_{i_1 \dots i_{2n-2}}, \quad (11) \\ f_{i_1 \dots i_{2n-2}} &= n_{i_1} \partial_1 n_{i_2} \partial_2 n_{i_3} \dots \partial_{2n-3} n_{i_{2n-2}}, \\ A_{2n-3} &= \frac{(n-2)!}{2\pi^{(n-1)}}, \end{aligned}$$

with the anti-symmetric tensor $\epsilon^{i_1 \dots i_{2n-2}}$ satisfying $\epsilon^{12 \dots 2n-2} = 1$. The vector $\mathbf{p} = (p_1, p_2, \dots, p_{2n-3})^T$ specifies a point on a $(2n-3)$ -dimensional sphere which encloses the EP n in the momentum space. The resultant winding number W_{2n-3} topologically characterizes a manifold of generic EP n s whose codimension is $2n-2$.

Generalizing Eq. (5), we provide an n -band toy model hosting a generic EP n . The Hamiltonian reads

$$H(\mathbf{k}) = \begin{pmatrix} 0 & 1 & & 0 \\ \vdots & \ddots & \ddots & \\ 0 & & 0 & 1 \\ z_{n-1} & \dots & z_1 & 0 \end{pmatrix} \quad (12)$$

with $z_j = k_{2j-1} + ik_{2j}$ ($j = 1, \dots, n-1$). The resultant vector of this toy model is obtained as (see Sec. S3 of SM [102])

$$R_{2j-1} = \alpha_{n,j} k_{2j-1}, \quad (13)$$

$$R_{2j} = \alpha_{n,j} k_{2j}, \quad (14)$$

with $\alpha_{n,j} = (-1)^{j(n+1)} (n!)^{j+1} (n-1-j)!$. Thus, this lone EP n at $\mathbf{k} = 0$ is characterized by the winding number $W_{2n-3} = 1$. Replacing $z_1 \rightarrow (k_1 \pm ik_2)^m$ yields a toy model hosting an EP n with $W_{2n-3} = \pm m$ ($m = 1, 2, \dots$), which we explicitly calculate in Sec. S4 of SM [102].

The $(2n-3)$ -dimensional resultant winding number W_{2n-3} leads to the doubling theorem of generic EP n s for an arbitrary n -band model in the $(2n-2)$ -dimensional BZ. In a similar way to the case of $n=3$ (see Sec. IIC), the sum of W_{2n-3} is deformed into an integral over the ‘‘boundary’’ of the BZ (∂BZ). The integral over ∂BZ vanishes due to the periodicity and the orientability of the BZ. This fact $\sum_I W_{2n-3I} = 0$ constitutes the doubling theorem: an EP n with $W_{2n-3} = 1$ must be accompanied by an EP n with $W_{2n-3} = -1$ in the BZ.

IV. SYMMETRY-PROTECTED EP n IN $n-1$ DIMENSIONS

The above topological characterization of EP n s can be extended to systems with symmetry. We emphasize that the following argument for systems with PT -symmetry

applies directly to systems with pseudo-Hermiticity, CP -symmetry, or chiral symmetry.

A PT -symmetric Hamiltonian satisfies

$$U_{PT} H^*(\mathbf{k}) U_{PT}^\dagger = H(\mathbf{k}), \quad (15)$$

where ‘‘*’’ denotes complex conjugation, and the unitary matrix U_{PT} satisfies $U_{PT} U_{PT}^* = \mathbb{1}$. The above constraint implies that the corresponding characteristic polynomial $P(\lambda, \mathbf{k})$ takes the form

$$\begin{aligned} P(\lambda) &= \det[U_{PT} H^*(\mathbf{k}) U_{PT}^\dagger - \lambda \mathbb{1}] \\ &= \det[H^*(\mathbf{k}) - \lambda \mathbb{1}] \\ &= [P(\lambda^*)]^*. \end{aligned} \quad (16)$$

Namely, $P(\lambda)$ is a polynomial with real coefficients. Its n -tuple root is captured by the vanishing resultant vector defined as

$$\mathbf{R} = (r_1, r_2, \dots, r_{n-1})^T, \quad (17)$$

$$r_j(\mathbf{k}) = \text{Res}[\partial_\lambda^{n-1-j} P, \partial_\lambda^{n-1} P], \quad (18)$$

with $j = 1, 2, \dots, n-1$. We note that for polynomials with real coefficients, the resultants $r_j(\mathbf{k})$ are real. Therefore, $\mathbf{R} = 0$ amounts to $n-1$ real constraints, which means that the codimension of the symmetry-protected EP n s is $c = n-1$. Namely, symmetry-protected EP n s with PT -symmetry are stable against perturbations preserving the relevant symmetry in $n-1$ dimensions. In D dimensions ($D > n-1$), EP n s form a $(D-n+1)$ -dimensional manifold [59, 60].

The symmetry-protected EP n s in $n-1$ dimensions ($n = 2, 3, 4, \dots$) may possess nontrivial topology of the map from the $(n-2)$ -dimensional sphere around the EP n in the parameter space to the $(n-1)$ -dimensional normalized resultant vector $\mathbf{n} = \mathbf{R}/\sqrt{\mathbf{R} \cdot \mathbf{R}}$. Such maps are topologically classified as (see Sec. 4.1 of Ref. [103])

$$\pi_{n-2}(S^{n-2}) = \mathbb{Z}, \quad (19)$$

where the invariant is characterized by the winding number W_{n-2}

$$\begin{aligned} W_{n-2} &= \frac{\epsilon^{i_1 \dots i_{n-1}}}{A_{n-2}} \int d^{n-2} \mathbf{p} f_{i_1 \dots i_{n-1}}, \quad (20) \\ f_{i_1 \dots i_{n-1}} &= n_{i_1} \partial_1 n_{i_2} \partial_2 n_{i_3} \dots \partial_{n-2} n_{i_{n-1}}, \end{aligned}$$

with the area of the $(n-2)$ -dimensional sphere A_{n-2} given by

$$\begin{aligned} A_{2m-1} &= \frac{2\pi^m}{(m-1)!}, \quad (21) \\ A_{2m-2} &= \frac{2^{2m-1} \pi^{m-1} (m-1)!}{(2m-2)!}, \end{aligned}$$

for $m = 1, 2, \dots$. The vector $\mathbf{p} = (p_1, p_2, \dots, p_{n-2})^T$ specifies a point on a $(n-2)$ -dimensional sphere which encloses the EP n in the momentum space. The resultant

winding number W_{n-2} topologically characterizes a manifold of symmetry-protected EPns whose codimension is $n - 1$.

We provide an n -band toy model hosting a symmetry-protected EPn. The Hamiltonian reads

$$H(\mathbf{k}) = \begin{pmatrix} 0 & 1 & 0 \\ \vdots & \ddots & \ddots \\ 0 & 0 & 1 \\ z_{n-1} & \cdots & z_1 & 0 \end{pmatrix}, \quad (22)$$

with $z_j = k_j$ [$z_j = (-1)^j k_j$] ($j = 1, 2, \dots, n$) for odd [even] n . This Hamiltonian is an $n \times n$ -matrix with real entries, satisfying PT -symmetry with $U_{PT} = \mathbb{1}$ [see Eq. (15)]. As shown in Sec. S3 of SM [102], the resultant vector is given by

$$R_j = |\alpha_{n,j}| k_j, \quad (23)$$

$$\alpha_{n,j} = (-1)^{j(n+1)} (n!)^{j+1} (n-1-j)!,$$

with real numbers $\alpha_{n,j}$. Thus, the symmetry-protected EPn emerging in the toy model [Eq. (22)] is characterized by $W_{n-2} = 1$. The replacement $z_1 + iz_2 \rightarrow (q_1 \pm iq_2)^m$ yields a toy model that hosts an EPn with $W_{n-2} = \pm m$ ($m = 1, 2, \dots$). Here, q 's are defined as $q_j = k_j$ [$q_j = (-1)^j k_j$] for odd [even] n .

The $(n-2)$ -dimensional resultant winding number leads to the doubling theorem of EPns for an arbitrary PT -symmetric n -band model in the $(n-1)$ -dimensional BZ. In a similar way to the case of generic EP3s [see Eq. (7)], the sum of W_{n-2} is written as an integral over the ‘‘boundary’’ of the BZ (∂BZ). This integral over ∂BZ vanishes due to the periodicity and the orientability of the BZ. This fact $\sum_I W_{n-2I} = 0$ constitutes the doubling theorem: an EPn with $W_{n-2} = 1$ must be accompanied by an EPn with $W_{n-2} = -1$ in the BZ.

We finish this section by extensions to systems with pseudo-Hermiticity, CP -symmetry, or chiral symmetry. Pseudo-Hermiticity is written as

$$U_{\text{pH}} H(\mathbf{k}) U_{\text{pH}}^\dagger = H^\dagger(\mathbf{k}), \quad (24)$$

for a unitary matrix satisfying $U_{\text{pH}}^2 = \mathbb{1}$. Under pseudo-Hermiticity, the characteristic polynomial $P(\lambda)$ ($\lambda \in \mathbb{R}$) satisfies Eq. (16). Hence the argument for the PT -symmetric case applies directly.

CP -symmetry and chiral symmetry are respectively written as

$$U_{CP} H^*(\mathbf{k}) U_{CP}^\dagger = -H(\mathbf{k}), \quad (25)$$

$$U_c H^\dagger(\mathbf{k}) U_c^\dagger = -H(\mathbf{k}), \quad (26)$$

where U_{CP} (U_c) is a unitary matrix satisfying $U_{CP} U_{CP}^* = \mathbb{1}$ ($U_c^2 = \mathbb{1}$). By the identification $H'(\mathbf{k}) = iH(\mathbf{k})$, Eq. (25) [Eq. (26)] coincides with the constraint of PT -symmetry Eq. (16) [pseudo-Hermiticity Eq. (24)]. Hence the argument of the PT -symmetric case applies to both CP - and chiral symmetry as well.

V. DISCUSSION

In this paper, we have systematically characterized the Abelian topology of generic EPns and symmetry-protected EPns in arbitrary dimensions [see Table I]. Specifically, introducing resultant winding numbers, we have characterized the topology of generic EPns in $2n-2$ dimensions as well as symmetry-protected EPns in $n-1$ dimensions with PT -, CP -, pseudo-Hermiticity or chiral symmetry. In a D -dimensional parameter space with $D \geq c$, the resultant winding number characterizes a $(D-c)$ -dimensional manifold of generic [symmetry-protected] EPns, whose codimension is $c = 2n-2$ [$c = n-1$]. The introduced winding number leads to concomitant doubling theorems for both generic and symmetry-protected EPns appearing in n -band models.

We note that Ref. [97] also modified the resultant winding number for PT -symmetry-protected EP3 introduced in Ref. [59]. The novelty of our results is further generalizing the resultant winding numbers for both generic and symmetry-protected EPn for arbitrary n . These resultant winding numbers are verified by constructing toy models of generic and symmetry-protected EPn for arbitrary n . These results demonstrate the usefulness of the choice of resultants defined in Eqs. (8) and (17) which also differentiates from the previous work [97].

Our systematic characterization of the topological nature of EPns increases the fundamental understanding of non-Hermitian multiband structures of direct physical importance. The stability of generic EP3s in four dimensions will be of importance in non-Hermitian Floquet systems, where periodic driving effectively induces a fourth dimension. Going beyond Bloch Hamiltonians, recent studies show that multifold EPs scaling with system sizes have been reported in, e.g., the Hatano-Nelson model, paving the way to realize topologically stable EPns for any n by increasing system sizes. Concerning symmetry-protected EPns, our topological classification has important consequences already in two and three dimensions. While the previous work has characterized symmetry-protected EPs up to third order, our general argument applies to pertinent EP4s in three dimensions. Our result makes their topological classification directly relevant to three-dimensional photonic crystals, where PT symmetry can be implemented as a perfect balance between gain and loss. Furthermore, both symmetry-protected EP3s and EP4s have been experimentally realized in nitrogen-vacancy spin systems [93], single-photon setups [98] and correlated quantum many-body systems [91], showcasing the breadth of applications in numerous physical systems.

Beyond experimental implications, one natural continuation from a theoretical point of view is to investigate the interplay between the Abelian and non-Abelian topology in the characterization of EPns. We expect non-Abelian contributions to appear when additional bands are added, i.e., when EPns are studied in m -band models, for some integer $m > n$. Such a classification scheme is expected to include braiding of the complex eigenvalues

around EPns.

The Abelian framework outlined here guarantees the topological stability of EPns and serves as a robust cornerstone in the continued unraveling and understanding of the intriguing properties of the non-Hermitian topological band theory.

ACKNOWLEDGMENTS

T.Y. thanks Pierre Delplace for collaboration in the previous work [59]. T.Y. also thanks Guancong Ma for fruitful discussions of an acoustic system. M.S. acknowledges fruitful discussions with Anton Montag.

This work is supported by JSPS KAKENHI Grant Nos. JP21K13850, JP23KK0247, JSPS Bilateral Program No. JPJSBP120249925, and the Swedish Research Council (grant 2018-00313), the Wallenberg Academy Fellows program of the Knut and Alice Wallenberg Foundation (grant 2018.0460) and the Göran Gustafsson Foundation for Research in Natural Sciences and Medicine. L.R. is supported by the Knut and Alice Wallenberg Foundation under Grant No. 2017.0157. M.S. is supported by the Swedish Research Council (VR) under grant No. 2024-00272. T.Y. is grateful for the support from the ETH Pauli Center for Theoretical Studies and the Grant from Yamada Science Foundation.

-
- [1] X. Wan, A. M. Turner, A. Vishwanath, and S. Y. Savrasov, Topological semimetal and Fermi-arc surface states in the electronic structure of pyrochlore iridates, *Phys. Rev. B* **83**, 205101 (2011).
- [2] A. A. Burkov and L. Balents, Weyl Semimetal in a Topological Insulator Multilayer, *Phys. Rev. Lett.* **107**, 127205 (2011).
- [3] M. A. Silaev and G. E. Volovik, Topological Fermi arcs in superfluid ^3He , *Phys. Rev. B* **86**, 214511 (2012).
- [4] A. M. Turner, A. Vishwanath, and C. O. Head, Beyond band insulators: topology of semimetals and interacting phases, *Topological Insulators* **6**, 293 (2013).
- [5] B. Yan and C. Felser, Topological Materials: Weyl Semimetals, *Annual Review of Condensed Matter Physics* **8**, 337 (2017).
- [6] S.-Y. Xu, I. Belopolski, N. Alidoust, M. Neupane, G. Bian, C. Zhang, R. Sankar, G. Chang, Z. Yuan, C.-C. Lee, S.-M. Huang, H. Zheng, J. Ma, D. S. Sanchez, B. Wang, A. Bansil, F. Chou, P. P. Shibayev, H. Lin, S. Jia, and M. Z. Hasan, Discovery of a Weyl fermion semimetal and topological Fermi arcs, *Science* **349**, 613 (2015).
- [7] B. Q. Lv, H. M. Weng, B. B. Fu, X. P. Wang, H. Miao, J. Ma, P. Richard, X. C. Huang, L. X. Zhao, G. F. Chen, Z. Fang, X. Dai, T. Qian, and H. Ding, Experimental Discovery of Weyl Semimetal TaAs, *Phys. Rev. X* **5**, 031013 (2015).
- [8] X. Huang, L. Zhao, Y. Long, P. Wang, D. Chen, Z. Yang, H. Liang, M. Xue, H. Weng, Z. Fang, X. Dai, and G. Chen, Observation of the Chiral-Anomaly-Induced Negative Magnetoresistance in 3D Weyl Semimetal TaAs, *Phys. Rev. X* **5**, 031023 (2015).
- [9] H. Weyl, Elektron und Gravitation. I, *Zeitschrift für Physik* **56**, 330 (1929).
- [10] H. Yang, Y. Sun, Y. Zhang, W.-J. Shi, S. S. P. Parkin, and B. Yan, Topological Weyl semimetals in the chiral antiferromagnetic materials Mn_3Ge and Mn_3Sn , *New Journal of Physics* **19**, 015008 (2017).
- [11] T. Higo, D. Qu, Y. Li, C. L. Chien, Y. Otani, and S. Nakatsuji, Anomalous Hall effect in thin films of the Weyl antiferromagnet Mn_3Sn , *Applied Physics Letters* **113**, 202402 (2018).
- [12] T. Matsuda, N. Kanda, T. Higo, N. P. Armitage, S. Nakatsuji, and R. Matsunaga, Room-temperature terahertz anomalous Hall effect in Weyl antiferromagnet Mn_3Sn thin films, *Nature Communications* **11**, 909 (2020).
- [13] J. L. Mañes, Existence of bulk chiral fermions and crystal symmetry, *Phys. Rev. B* **85**, 155118 (2012).
- [14] B. Bradlyn, J. Cano, Z. Wang, M. G. Vergniory, C. Felser, R. J. Cava, and B. A. Bernevig, Beyond Dirac and Weyl fermions: Unconventional quasiparticles in conventional crystals, *Science* **353**, aaf5037 (2016).
- [15] H. Weng, C. Fang, Z. Fang, and X. Dai, Coexistence of Weyl fermion and massless triply degenerate nodal points, *Phys. Rev. B* **94**, 165201 (2016).
- [16] G. Chang, S.-Y. Xu, B. J. Wieder, D. S. Sanchez, S.-M. Huang, I. Belopolski, T.-R. Chang, S. Zhang, A. Bansil, H. Lin, and M. Z. Hasan, Unconventional Chiral Fermions and Large Topological Fermi Arcs in RhSi, *Phys. Rev. Lett.* **119**, 206401 (2017).
- [17] P. Tang, Q. Zhou, and S.-C. Zhang, Multiple Types of Topological Fermions in Transition Metal Silicides, *Phys. Rev. Lett.* **119**, 206402 (2017).
- [18] F. Flicker, F. de Juan, B. Bradlyn, T. Morimoto, M. G. Vergniory, and A. G. Grushin, Chiral optical response of multifold fermions, *Phys. Rev. B* **98**, 155145 (2018).
- [19] M.-A. Sánchez-Martínez, F. de Juan, and A. G. Grushin, Linear optical conductivity of chiral multifold fermions, *Phys. Rev. B* **99**, 155145 (2019).
- [20] L. Z. Maulana, K. Manna, E. Uykur, C. Felser, M. Dressel, and A. V. Pronin, Optical conductivity of multifold fermions: The case of RhSi, *Phys. Rev. Res.* **2**, 023018 (2020).
- [21] Z. S. Gao, X.-J. Gao, W.-Y. He, X. Y. Xu, T. K. Ng, and K. T. Law, Topological superconductivity in multifold fermion metals, *Quantum Frontiers* **1**, 3 (2022).
- [22] H.-C. Hsu, J.-S. You, J. Ahn, and G.-Y. Guo, Nonlinear photoconductivities and quantum geometry of chiral multifold fermions, *Phys. Rev. B* **107**, 155434 (2023).
- [23] F. Balduini, A. Molinari, L. Rocchino, V. Hasse, C. Felser, M. Sousa, C. Zota, H. Schmid, A. G. Grushin, and B. Gotsmann, Intrinsic negative magnetoresistance from the chiral anomaly of multifold fermions, *Nature Communications* **15**, 6526 (2024).
- [24] Z. Rao, H. Li, T. Zhang, S. Tian, C. Li, B. Fu, C. Tang, L. Wang, Z. Li, W. Fan, J. Li, Y. Huang, Z. Liu, Y. Long, C. Fang, H. Weng, Y. Shi, H. Lei, Y. Sun,

- T. Qian, and H. Ding, Observation of unconventional chiral fermions with long Fermi arcs in CoSi, *Nature* **567**, 496 (2019).
- [25] D. Takane, Z. Wang, S. Souma, K. Nakayama, T. Nakamura, H. Oinuma, Y. Nakata, H. Iwasawa, C. Cacho, T. Kim, K. Horiba, H. Kumigashira, T. Takahashi, Y. Ando, and T. Sato, Observation of Chiral Fermions with a Large Topological Charge and Associated Fermi-Arc Surface States in CoSi, *Phys. Rev. Lett.* **122**, 076402 (2019).
- [26] N. B. M. Schröter, D. Pei, M. G. Vergniory, Y. Sun, K. Manna, F. de Juan, J. A. Krieger, V. Süß, M. Schmidt, P. Dudin, B. Bradlyn, T. K. Kim, T. Schmitt, C. Cacho, C. Felser, V. N. Strocov, and Y. Chen, Chiral topological semimetal with multifold band crossings and long Fermi arcs, *Nature Physics* **15**, 759 (2019).
- [27] D. S. Sanchez, I. Belopolski, T. A. Cochran, X. Xu, J.-X. Yin, G. Chang, W. Xie, K. Manna, V. Süß, C.-Y. Huang, N. Alidoust, D. Multer, S. S. Zhang, N. Shumiya, X. Wang, G.-Q. Wang, T.-R. Chang, C. Felser, S.-Y. Xu, S. Jia, H. Lin, and M. Z. Hasan, Topological chiral crystals with helicoid-arc quantum states, *Nature* **567**, 500 (2019).
- [28] Y. C. Hu and T. L. Hughes, Absence of topological insulator phases in non-Hermitian PT -symmetric Hamiltonians, *Phys. Rev. B* **84**, 153101 (2011).
- [29] K. Esaki, M. Sato, K. Hasebe, and M. Kohmoto, Edge states and topological phases in non-Hermitian systems, *Phys. Rev. B* **84**, 205128 (2011).
- [30] N. Hatano and D. R. Nelson, Localization Transitions in Non-Hermitian Quantum Mechanics, *Phys. Rev. Lett.* **77**, 570 (1996).
- [31] N. Hatano and D. R. Nelson, Vortex pinning and non-Hermitian quantum mechanics, *Phys. Rev. B* **56**, 8651 (1997).
- [32] T. E. Lee, Anomalous Edge State in a Non-Hermitian Lattice, *Phys. Rev. Lett.* **116**, 133903 (2016).
- [33] Z. Gong, S. Higashikawa, and M. Ueda, Zeno Hall Effect, *Phys. Rev. Lett.* **118**, 200401 (2017).
- [34] V. M. Martinez Alvarez, J. E. Barrios Vargas, and L. E. F. Foa Torres, Non-Hermitian robust edge states in one dimension: Anomalous localization and eigenspace condensation at exceptional points, *Phys. Rev. B* **97**, 121401 (2018).
- [35] S. Yao and Z. Wang, Edge States and Topological Invariants of Non-Hermitian Systems, *Phys. Rev. Lett.* **121**, 086803 (2018).
- [36] S. Yao, F. Song, and Z. Wang, Non-Hermitian Chern Bands, *Phys. Rev. Lett.* **121**, 136802 (2018).
- [37] F. K. Kunst, E. Edvardsson, J. C. Budich, and E. J. Bergholtz, Biorthogonal Bulk-Boundary Correspondence in Non-Hermitian Systems, *Phys. Rev. Lett.* **121**, 026808 (2018).
- [38] K. Yokomizo and S. Murakami, Non-Bloch Band Theory of Non-Hermitian Systems, *Phys. Rev. Lett.* **123**, 066404 (2019).
- [39] C. H. Lee and R. Thomale, Anatomy of skin modes and topology in non-Hermitian systems, *Phys. Rev. B* **99**, 201103 (2019).
- [40] D. S. Borgnia, A. J. Kruchkov, and R.-J. Slager, Non-Hermitian Boundary Modes and Topology, *Phys. Rev. Lett.* **124**, 056802 (2020).
- [41] H.-G. Zirnstein, G. Refael, and B. Rosenow, Bulk-Boundary Correspondence for Non-Hermitian Hamiltonians via Green Functions, *Phys. Rev. Lett.* **126**, 216407 (2021).
- [42] K. Zhang, Z. Yang, and C. Fang, Correspondence between Winding Numbers and Skin Modes in Non-Hermitian Systems, *Phys. Rev. Lett.* **125**, 126402 (2020).
- [43] N. Okuma, K. Kawabata, K. Shiozaki, and M. Sato, Topological Origin of Non-Hermitian Skin Effects, *Phys. Rev. Lett.* **124**, 086801 (2020).
- [44] F. Song, S. Yao, and Z. Wang, Non-Hermitian Skin Effect and Chiral Damping in Open Quantum Systems, *Phys. Rev. Lett.* **123**, 170401 (2019).
- [45] L. Xiao, T. Deng, K. Wang, G. Zhu, Z. Wang, W. Yi, and P. Xue, Non-Hermitian bulk-boundary correspondence in quantum dynamics, *Nat. Phys.* **16**, 761 (2020).
- [46] Z. Gong, Y. Ashida, K. Kawabata, K. Takasan, S. Higashikawa, and M. Ueda, Topological Phases of Non-Hermitian Systems, *Phys. Rev. X* **8**, 031079 (2018).
- [47] K. Kawabata, S. Higashikawa, Z. Gong, Y. Ashida, and M. Ueda, Topological unification of time-reversal and particle-hole symmetries in non-Hermitian physics, *Nat. Commun.* **10**, 297 (2019).
- [48] K. Kawabata, K. Shiozaki, M. Ueda, and M. Sato, Symmetry and Topology in Non-Hermitian Physics, *Phys. Rev. X* **9**, 041015 (2019).
- [49] H. Zhou and J. Y. Lee, Periodic table for topological bands with non-Hermitian symmetries, *Phys. Rev. B* **99**, 235112 (2019).
- [50] E. J. Bergholtz, J. C. Budich, and F. K. Kunst, Exceptional topology of non-Hermitian systems, *Rev. Mod. Phys.* **93**, 015005 (2021).
- [51] Y. Ashida, Z. Gong, and M. Ueda, Non-Hermitian physics, *Advances in Physics* **69**, 249 (2020).
- [52] N. Okuma and M. Sato, Non-Hermitian Topological Phenomena: A Review, *Annual Review of Condensed Matter Physics* **14**, 83 (2023).
- [53] R. Lin, T. Tai, L. Li, and C. H. Lee, Topological non-Hermitian skin effect, *Frontiers of Physics* **18**, 53605 (2023).
- [54] T. Katō, *Perturbation theory for linear operators*, Vol. 132 (Springer, 1966).
- [55] H. Shen, B. Zhen, and L. Fu, Topological Band Theory for Non-Hermitian Hamiltonians, *Phys. Rev. Lett.* **120**, 146402 (2018).
- [56] K. Kawabata, T. Bessho, and M. Sato, Classification of Exceptional Points and Non-Hermitian Topological Semimetals, *Phys. Rev. Lett.* **123**, 066405 (2019).
- [57] Z. Yang, A. P. Schnyder, J. Hu, and C.-K. Chiu, Fermion Doubling Theorems in Two-Dimensional Non-Hermitian Systems for Fermi Points and Exceptional Points, *Phys. Rev. Lett.* **126**, 086401 (2021).
- [58] G. Demange and E.-M. Graefe, Signatures of three coalescing eigenfunctions, *Journal of Physics A: Mathematical and Theoretical* **45**, 025303 (2011).
- [59] P. Delplace, T. Yoshida, and Y. Hatsugai, Symmetry-Protected Multifold Exceptional Points and their Topological Characterization, *Phys. Rev. Lett.* **127**, 186602 (2021).
- [60] I. Mandal and E. J. Bergholtz, Symmetry and Higher-Order Exceptional Points, *Phys. Rev. Lett.* **127**, 186601 (2021).
- [61] S. Sayyad and F. K. Kunst, Realizing exceptional points of any order in the presence of symmetry, *Phys. Rev.*

- Res. **4**, 023130 (2022).
- [62] J. L. K. König, K. Yang, J. C. Budich, and E. J. Bergholtz, Braid-protected topological band structures with unpaired exceptional points, *Phys. Rev. Res.* **5**, L042010 (2023).
- [63] K. Yang, Z. Li, J. L. K. König, L. Rødland, M. Stålhammar, and E. J. Bergholtz, Homotopy, symmetry, and non-Hermitian band topology, *Reports on Progress in Physics* **87**, 078002 (2024).
- [64] K. Yang and I. Mandal, Enhanced eigenvector sensitivity and algebraic classification of sublattice-symmetric exceptional points, *Phys. Rev. B* **107**, 144304 (2023).
- [65] A. Montag and F. K. Kunst, Symmetry-induced higher-order exceptional points in two dimensions, *Phys. Rev. Res.* **6**, 023205 (2024).
- [66] I. Rotter, A non-Hermitian Hamilton operator and the physics of open quantum systems, *J. Phys. A* **42**, 153001 (2009).
- [67] M. V. Berry, Physics of Nonhermitian Degeneracies, *Czech. J. Phys.* **54**, 1039 (2004).
- [68] W. D. Heiss, The physics of exceptional points, *Journal of Physics A: Mathematical and Theoretical* **45**, 444016 (2012).
- [69] Y. Xu, S.-T. Wang, and L.-M. Duan, Weyl Exceptional Rings in a Three-Dimensional Dissipative Cold Atomic Gas, *Phys. Rev. Lett.* **118**, 045701 (2017).
- [70] V. Kozii and L. Fu, Non-Hermitian topological theory of finite-lifetime quasiparticles: Prediction of bulk Fermi arc due to exceptional point, *Phys. Rev. B* **109**, 235139 (2024).
- [71] K. Takata and M. Notomi, Photonic Topological Insulating Phase Induced Solely by Gain and Loss, *Phys. Rev. Lett.* **121**, 213902 (2018).
- [72] A. A. Zyuzin and A. Y. Zyuzin, Flat band in disorder-driven non-Hermitian Weyl semimetals, *Phys. Rev. B* **97**, 041203 (2018).
- [73] T. Yoshida, R. Peters, and N. Kawakami, Non-Hermitian perspective of the band structure in heavy-fermion systems, *Phys. Rev. B* **98**, 035141 (2018).
- [74] T. Yoshida, R. Okugawa, and Y. Hatsugai, Discriminant indicators with generalized inversion symmetry, *Phys. Rev. B* **105**, 085109 (2022).
- [75] At n -fold band-touching point of Hermitian cases, the $n \times n$ Hamiltonian should be proportional to the identity matrix, which leads to $n^2 - 1$ constraints. We note that $n \times n$ Hamiltonians are described by n^2 real numbers. The diagonal elements are described by n real numbers. The off-diagonal elements are described by $n^2 - n$ real numbers because they are complex but related to each other because of Hermiticity. Therefore, $n^2 - 1$ parameters need to be tuned for n -fold band touching
- [76] J. C. Budich, J. Carlström, F. K. Kunst, and E. J. Bergholtz, Symmetry-protected nodal phases in non-Hermitian systems, *Phys. Rev. B* **99**, 041406 (2019).
- [77] R. Okugawa and T. Yokoyama, Topological exceptional surfaces in non-Hermitian systems with parity-time and parity-particle-hole symmetries, *Phys. Rev. B* **99**, 041202 (2019).
- [78] T. Yoshida, R. Peters, N. Kawakami, and Y. Hatsugai, Symmetry-protected exceptional rings in two-dimensional correlated systems with chiral symmetry, *Phys. Rev. B* **99**, 121101 (2019).
- [79] H. Zhou, J. Y. Lee, S. Liu, and B. Zhen, Exceptional surfaces in PT-symmetric non-Hermitian photonic systems, *Optica* **6**, 190 (2019).
- [80] T. Yoshida and Y. Hatsugai, Exceptional rings protected by emergent symmetry for mechanical systems, *Phys. Rev. B* **100**, 054109 (2019).
- [81] K. Kimura, T. Yoshida, and N. Kawakami, Chiral-symmetry protected exceptional torus in correlated nodal-line semimetals, *Phys. Rev. B* **100**, 115124 (2019).
- [82] T. Yoshida, R. Peters, N. Kawakami, and Y. Hatsugai, Exceptional band touching for strongly correlated systems in equilibrium, *Progress of Theoretical and Experimental Physics* **2020**, 12A109 (2020).
- [83] M. Stålhammar and E. J. Bergholtz, Classification of exceptional nodal topologies protected by \mathcal{PT} symmetry, *Phys. Rev. B* **104**, L201104 (2021).
- [84] S. Sayyad, M. Stålhammar, L. Rødland, and F. K. Kunst, Symmetry-protected exceptional and nodal points in non-Hermitian systems, *SciPost Phys.* **15**, 200 (2023).
- [85] Z. Lin, A. Pick, M. Lončar, and A. W. Rodriguez, Enhanced Spontaneous Emission at Third-Order Dirac Exceptional Points in Inverse-Designed Photonic Crystals, *Phys. Rev. Lett.* **117**, 107402 (2016).
- [86] J. Schnabel, H. Cartarius, J. Main, G. Wunner, and W. D. Heiss, \mathcal{PT} -symmetric waveguide system with evidence of a third-order exceptional point, *Phys. Rev. A* **95**, 053868 (2017).
- [87] J. Wiersig, Revisiting the hierarchical construction of higher-order exceptional points, *Phys. Rev. A* **106**, 063526 (2022).
- [88] Y.-X. Xiao, K. Ding, R.-Y. Zhang, Z. H. Hang, and C. T. Chan, Exceptional points make an astroid in non-Hermitian Lieb lattice: Evolution and topological protection, *Phys. Rev. B* **102**, 245144 (2020).
- [89] N. Hatano, Exceptional points of the Lindblad operator of a two-level system, *Molecular Physics* **117**, 2121 (2019).
- [90] S. Khandelwal, N. Brunner, and G. Haack, Signatures of Liouvillian Exceptional Points in a Quantum Thermal Machine, *PRX Quantum* **2**, 040346 (2021).
- [91] L. Crippa, J. C. Budich, and G. Sangiovanni, Fourth-order exceptional points in correlated quantum many-body systems, *Phys. Rev. B* **104**, L121109 (2021).
- [92] J. T. Gohsrich, J. Fauman, and F. K. Kunst, Exceptional points of any order in a generalized Hatano-Nelson model, *arXiv:2403.12018* (2024).
- [93] Y. Wu, Y. Wang, X. Ye, W. Liu, Z. Niu, C.-K. Duan, Y. Wang, X. Rong, and J. Du, Third-order exceptional line in a nitrogen-vacancy spin system, *Nature Nanotechnology* **19**, 160 (2024).
- [94] K. Bai, J.-Z. Li, T.-R. Liu, L. Fang, D. Wan, and M. Xiao, Nonlinear Exceptional Points with a Complete Basis in Dynamics, *Phys. Rev. Lett.* **130**, 266901 (2023).
- [95] Q. Liu, D. A. Kessler, and E. Barkai, Designing exceptional-point-based graphs yielding topologically guaranteed quantum search, *Phys. Rev. Res.* **5**, 023141 (2023).
- [96] W. Tang, X. Jiang, K. Ding, Y.-X. Xiao, Z.-Q. Zhang, C. T. Chan, and G. Ma, Exceptional nexus with a hybrid topological invariant, *Science* **370**, 1077 (2020).
- [97] W. Tang, K. Ding, and G. Ma, Realization and topological properties of third-order exceptional lines embedded in exceptional surfaces, *Nature Communications* **14**, 6660 (2023).
- [98] K. Wang, L. Xiao, H. Lin, W. Yi, E. J. Bergholtz, and

- P. Xue, Experimental simulation of symmetry-protected higher-order exceptional points with single photons, *Science Advances* **9**, eadi0732 (2023).
- [99] H. Hodaiei, A. U. Hassan, S. Wittek, H. Garcia-Gracia, R. El-Ganainy, D. N. Christodoulides, and M. Khajavikhan, Enhanced sensitivity at higher-order exceptional points, *Nature* **548**, 187 (2017).
- [100] In principle, an $n \times n$ Hamiltonian can be diagonalizable. This case, however, requires additional tuning of $\mathcal{O}(n^2)$ parameters; the generic form of a degenerate Hamiltonian is a Jordan block.
- [101] The resultant of two polynomials is defined as the determinant of the Sylvester matrix, a matrix whose elements are coefficients of these polynomials. The resultant vanishes when these polynomials have a common root
- [102] Supplemental Material for details of resultants, characterization of a generic EP3 in an acoustic system, and toy models of EPns for arbitrary n
- [103] A. Hatcher, *Algebraic topology* (Cambridge University Press, Cambridge, 2002).
- [104] The topological invariant W_3 can be regarded as an extension of the one-dimensional winding number of the discriminant that characterizes the Abelian topology of EP2s [57].
- [105] This resultant approach cannot be directly applied to Hermitian band-touching. This is because the resultant does not include information of wavefunctions whose topology protects Hermitian band-touching. For instance, 2-band touching corresponds to vanishing discriminant $\text{Res}[P(\lambda), \partial_\lambda P(\lambda)] = 0$. However, a Weyl node, Hermitian 2-band touching, cannot be captured by the winding of the discriminant because it is always real and non-negative
- [106] V. Mathai and G. C. Thiang, Differential Topology of Semimetals, *Communications in Mathematical Physics* **355**, 561 (2017).
- [107] V. Mathai and G. C. Thiang, Global topology of Weyl semimetals and Fermi arcs, *Journal of Physics A: Mathematical and Theoretical* **50**, 11LT01 (2017).
- [108] Mathematically, what is commonly denoted as the BZ boundary ∂BZ really is a double cover of a choice of $n - 1$ -skeleton of the n -dimensional BZ

Supplemental Materials:
Winding Topology of Multifold Exceptional Points

S1. EP n AND THE VANISHING RESULTANTS

For an $n \times n$ -Hamiltonian, the vanishing resultants indicate the emergence of an EP n . Specifically, we prove that the characteristic polynomial is written as

$$P(\lambda) = (-1)^n (\lambda - \epsilon_0)^n \quad (\text{S1})$$

with $\epsilon_0 \in \mathbb{C}$ if and only if

$$\begin{aligned} \text{Res}[P(\lambda), \partial_\lambda^{n-1} P(\lambda)] &= 0, \\ \text{Res}[\partial_\lambda^2 P(\lambda), \partial_\lambda^{n-1} P(\lambda)] &= 0, \\ &\vdots \\ \text{Res}[\partial_\lambda^{n-2} P(\lambda), \partial_\lambda^{n-1} P(\lambda)] &= 0 \end{aligned} \quad (\text{S2})$$

are satisfied.

A. A proof of Eq. (S1) \Rightarrow Eq. (S2)

When Eq. (S1) holds, we have

$$\partial_\lambda^l P(\lambda) = (-1)^n \frac{n!}{(n-l)!} (\lambda - \epsilon_0)^{n-l} \quad (\text{S3})$$

with $l = 0, 1, \dots, n-1$, indicating that $\partial_\lambda^l P(\lambda)$ and $\partial_\lambda^{l'} P(\lambda)$ have the common root $\lambda = \epsilon_0$ for $l, l' = 0, 1, \dots, n-1$. Thus, Eq. (S2) holds.

B. A proof of Eq. (S2) \Rightarrow Eq. (S1)

We consider the characteristic polynomial $P(\lambda)$ of degree n . Its $(n-1)$ -th derivative is linear, $\partial_\lambda^{n-1} P = c(\lambda - \epsilon_0)$ with some constant c , and thus has only one root $\lambda = \epsilon_0$. The vanishing resultants in Eq. (S2) imply that $P(\lambda)$ and all of its derivatives share a root with this linear polynomial. Since there is only one such root, P and all of its derivatives must have ϵ_0 as the root. For a polynomial of finite degree, this is only possible if there are no other roots, hence P has an n -tuple root at ϵ_0 .

Recalling that the leading coefficient of the characteristic polynomial is $(-1)^n$, we can fix the overall prefactor and obtain $P(\lambda) = (-1)^n (\lambda - \epsilon_0)^n$.

S2. EP3 IN A COUPLED ACOUSTIC CAVITY SYSTEM

Reference 96 reports that a coupled acoustic cavity system hosts EP3 in a four-dimensional parameter space. This section provides the details of its characterization based on our resultant winding number.

The coupled acoustic cavity system is described by the following effective Hamiltonian

$$H = (\omega_0 + i\gamma_0)\mathbb{1} + \kappa \begin{pmatrix} i\sqrt{2}(1 + \Lambda) & -1 & 0 \\ -1 & i\Xi & -1 \\ 0 & -1 & -i\sqrt{2}(1 + \Lambda) \end{pmatrix}, \quad (\text{S4})$$

with $\Xi = \delta_f + i\delta_A$ and $\Lambda = \delta_g + i\delta_B$ ($\delta_f, \delta_f, \delta_A, \delta_B \in \mathbb{R}$). Here, δ_A and δ_B (δ_g and δ_f) are detuning (gain or loss) of each cavity. Coupling between cavities is described by κ ($\kappa \in \mathbb{R}$). The onsite eigenfrequency and intrinsic loss are described by ω_0 and γ_0 ($\omega_0, \gamma_0 \in \mathbb{R}$), respectively. The experiment is carried out for $\omega_0 = 19,613$ rad/s and $\kappa = 49.9$ rad/s. The EP3 is characterized by analyzing the matrix in the second term scaled by κ .

The EP3 emerges at the origin of a four-dimensional space parameterized by $(\delta_f, \delta_A, \delta_g, \delta_B)$. Numerically computing the resultant winding number [Eq. (4)] yields $W_3 = 1$.

S3. RESULTANT OF A TOY MODEL OF EP n

We consider the following Hamiltonian of an $n \times n$ -matrix

$$H = \begin{pmatrix} 0 & 1 & & 0 \\ \vdots & \ddots & \ddots & \\ 0 & & 0 & 1 \\ z_{n-1} & \cdots & z_1 & 0 \end{pmatrix} \quad (\text{S5})$$

with z_j ($j = 1, \dots, n-1$) being functions of \mathbf{k} . The characteristic polynomial $P_n(\lambda) = \det[H - \mathbb{1}\lambda]$ is given by

$$P_n(\lambda) = (-1)^n \left[\lambda^n - (z_1 \lambda^{n-2} + z_2 \lambda^{n-3} + \cdots + z_{n-1-l} \lambda^l + \cdots + z_{n-1}) \right].$$

The above relation can be seen by noting the recurrence relation

$$P_n(\lambda) = -\lambda P_{n-1}(\lambda) + (-1)^{n-1} z_{n-1}, \quad (\text{S6})$$

and

$$P_2(\lambda) = \lambda^2 - z_1. \quad (\text{S7})$$

We note that $(n-1)$ -th derivative of $P_n(\lambda)$ is given by $\partial_\lambda^{(n-1)} P_n(\lambda) = (-1)^n n! \lambda$.

Let us consider two polynomials

$$f(x) = a_m x^m + a_{m-1} x^{m-1} + \cdots + a_0, \quad (\text{S8})$$

$$g(x) = b_1 x, \quad (\text{S9})$$

with coefficients $a_i, i = 1, \dots, m$ and b_1 . The resultant of these polynomials is given by

$$\text{Res}[f(x), g(x)] = (-1)^m b_1^m a_0, \quad (\text{S10})$$

which can be seen from a direct computation

$$\text{Res}[f(x), g(x)] = \det \begin{bmatrix} a_m & a_{m-1} & \cdots & a_1 & a_0 \\ b_1 & 0 & \cdots & 0 & 0 \\ 0 & b_1 & \cdots & 0 & 0 \\ 0 & 0 & \ddots & \vdots & \vdots \\ \vdots & & & 0 & b_1 & 0 \end{bmatrix}. \quad (\text{S11})$$

We apply this fact to the characteristic polynomial in Eq. (S6) with $\partial_\lambda^{n-1} P_n(\lambda) = (-1)^n n! \lambda$. Using Eq. (S10), we obtain

$$\text{Res}[\partial_\lambda^l P_n(\lambda), \partial_\lambda^{n-1} P_n(\lambda)] = (-1)^{(n+1)(l+1)} (n!)^{n-l} l! z_{n-1-l}, \quad (\text{S12})$$

which leads to

$$\begin{aligned} r_j &= \alpha_{n,j} z_j, \\ \alpha_{n,j} &= (-1)^{j(n+1)} (n!)^{j+1} (n-1-j)! . \end{aligned} \quad (\text{S13})$$

Therefore, specifying the momentum dependence of z_j , we obtain the specific form of the resultant vector.

For $z_j = k_{2j-1} + i k_{2j}$, the toy model of a general EP n , we obtain the resultant vector from the real and imaginary parts of r_j as

$$R_{2j-1} = \alpha_{n,j} k_{2j-1}, \quad (\text{S14})$$

$$R_{2j} = \alpha_{n,j} k_{2j}, \quad (\text{S15})$$

following Eq. (8).

For $z_j = (-1)^{j(n+1)} k_j$, the toy model of symmetry-protected EP n s, we construct the resultant vector from the real parts of r_j as

$$R_j = |\alpha_{n,j}| k_j, \quad (\text{S16})$$

following Eq. (17).

S4. TOY MODEL TAKING AN ARBITRARY W_{2n-3}

We prove that the EP n in toy model (S5) is characterized by $W_{2n-3} = \pm m$ ($m = 0, 1, 2, \dots$) for

$$z_1 = \begin{cases} k_1^2 + k_2^2 & \text{if } m = 0 \\ (k_1 \pm ik_2)^m & \text{otherwise,} \end{cases} \quad (\text{S17})$$

$$z_j = k_{2j-1} + ik_{2j} \quad (j = 2, \dots, n-1). \quad (\text{S18})$$

A. Case of positive W_{2n-3}

Firstly, we note that the winding number is computed from

$$W_{2n-3} = \sum_{\mathbf{n}(\mathbf{k}_l) = \mathbf{n}_0} \text{sgn}[J(\mathbf{k}_l)] \quad (\text{S19})$$

after fixing some arbitrary regular point \mathbf{n}_0 in the target space S^{2n-3} . The sum is over the preimage of this point, i.e., over \mathbf{k}_l satisfying $\mathbf{n}(\mathbf{k}_l) = \mathbf{n}_0$, and $\text{sgn}(x)$ takes 1 (-1) for $x > 0$ ($x < 0$). The Jacobian $J(\mathbf{k})$ is given by

$$J(\mathbf{k}) = \left| \frac{\partial(n_1, n_2, \dots, n_{2n-2})}{\partial(k_1, k_2, \dots, k_{2n-2})} \right|. \quad (\text{S20})$$

By making use of Eq. (S19), we compute the winding number. We take as the point \mathbf{n}_0 either the north or the south pole of the sphere, according to r 's giving $\mathbf{n}_0 = \text{sgn}(\alpha_{n1})(1, 0, \dots, 0)^T$. In this case, resultants

$$r_j = \begin{cases} \alpha_{n1}, & j = 1 \\ 0, & j = 2, \dots, n-1, \end{cases} \quad (\text{S21})$$

corresponds to constraints on z_j

$$z_j = \begin{cases} 1, & j = 1 \\ 0, & j = 2, \dots, n-1. \end{cases} \quad (\text{S22})$$

Thus, for

$$z_1 = (k_1 + ik_2)^m, \quad z_j = k_{2j-1} + ik_{2j} \quad (\text{S23})$$

with $m = 1, 2, \dots$ and $j = 2, \dots, n-1$, we find the preimages in terms of the the m -th root of unity

$$k_{l1} + ik_{l2} = e^{i\frac{2\pi l}{m}}, \quad k_{l3} = \dots = k_{l2n-2} = 0, \quad (\text{S24})$$

with $l = 0, \dots, m-1$.

From Eq. (S23), we have

$$\begin{aligned} \frac{\partial z_1}{\partial k_1} &= me^{-i\frac{2\pi l}{m}}, \\ \frac{\partial z_1}{\partial k_2} &= ime^{-i\frac{2\pi l}{m}}, \end{aligned} \quad (\text{S25})$$

for $\mathbf{k} = \mathbf{k}_l$.

Thus, for each l , we obtain the Jacobian $J(\mathbf{k}_l)$ from the real and imaginary parts of z_i as

$$J(\mathbf{k}_l) = \det \begin{bmatrix} J_{2 \times 2} & 0 & \dots & 0 \\ 0 & 1 & & \\ \vdots & & \ddots & \\ 0 & & & 1 \end{bmatrix}, \quad (\text{S26})$$

$$J_{2 \times 2} = \begin{pmatrix} m \cos\left(\frac{2\pi l}{m}\right) & -m \sin\left(\frac{2\pi l}{m}\right) \\ m \sin\left(\frac{2\pi l}{m}\right) & m \cos\left(\frac{2\pi l}{m}\right) \end{pmatrix}. \quad (\text{S27})$$

Thus, the sign of this Jacobian is always +1 for arbitrary l , which leads to

$$W_{2n-3} = \sum_{\mathbf{n}(\mathbf{k})=n_0} \text{sgn}[J(\mathbf{k})] = m \quad (\text{S28})$$

for $m = 1, 2, \dots$.

B. Case of negative W_{2n-3}

In a similar way, we can compute the winding number W_{2n-3} of negative values. The difference is the Jacobian. Because we have

$$\begin{aligned} \frac{\partial z_1}{\partial k_1} &= m e^{-i \frac{2\pi l}{m}}, \\ \frac{\partial z_1}{\partial k_2} &= -i m e^{-i \frac{2\pi l}{m}}, \end{aligned} \quad (\text{S29})$$

for $\mathbf{k} = \mathbf{k}_l$ ($l = 0, 1, \dots, m-1$), we obtain

$$J(\mathbf{k}_l) = \det \begin{bmatrix} J_{2 \times 2} & 0 & \cdots & 0 \\ 0 & 1 & & \\ \vdots & & \ddots & \\ 0 & & & 1 \end{bmatrix}, \quad (\text{S30})$$

$$J_{2 \times 2} = \begin{pmatrix} m \cos\left(\frac{2\pi l}{m}\right) & -m \sin\left(\frac{2\pi l}{m}\right) \\ -m \sin\left(\frac{2\pi l}{m}\right) & -m \cos\left(\frac{2\pi l}{m}\right) \end{pmatrix}. \quad (\text{S31})$$

Thus, the sign of this Jacobian is -1 for arbitrary l , which leads to

$$W_{2n-3} = -m \quad (\text{S32})$$

with $m = 1, 2, \dots$.

C. Case of zero W_{2n-3}

For the model with $m = 0$, we note that the vector \mathbf{R} does not cover the full sphere, since $\text{Im } r_1(\mathbf{k}) = 0$. The homotopy invariant of a non-surjective map is always zero. This can be seen by applying the summation formula Eq. (S19) to the empty preimage of any point with non-zero $R_2 = \text{Im } r_1$.